Europace (2014) **16**, 416–423
doi:10.1093/europace/eut349

Evolution and pharmacological modulation of the arrhythmogenic wave dynamics in canine pulmonary vein model

Michael A. Colman[1], Marta Varela[2], Jules C. Hancox[3], Henggui Zhang[1] and Oleg V. Aslanidi[2]*

[1]Biological Physics Group, School of Physics & Astronomy, University of Manchester, Manchester M13 9PL, UK; [2]Department of Biomedical Engineering, Division of Imaging Sciences & Biomedical Engineering, King's College London, St Thomas' Hospital, London SE1 7EH, UK; and [3]Department of Physiology & Pharmacology, School of Medical Science, University of Bristol, Bristol BS8 1TD, UK

Received 15 July 2013; accepted after revision 2 October 2013

Aims Atrial fibrillation (AF), the commonest cardiac arrhythmia, has been strongly linked with arrhythmogenic sources near the pulmonary veins (PVs), but underlying mechanisms are not fully understood. We aim to study the generation and sustenance of wave sources in a model of the PV tissue.

Methods and results A previously developed biophysically detailed three-dimensional canine atrial model is applied. Effects of AF-induced electrical remodelling are introduced based on published experimental data, as changes of ion channel currents (I_{CaL}, I_{K1}, I_{to}, and I_{Kur}), the action potential (AP) and cell-to-cell coupling levels. Pharmacological effects are introduced by blocking specific ion channel currents. A combination of electrical heterogeneity (AP tissue gradients of 5–12 ms) and anisotropy (conduction velocities of 0.75–1.25 and 0.21–0.31 m/s along and transverse to atrial fibres) can results in the generation of wave breaks in the PV region. However, a long wavelength (171 mm) prevents the wave breaks from developing into re-entry. Electrical remodelling leads to decreases in the AP duration, conduction velocity and wavelength (to 49 mm), such that re-entry becomes sustained. Pharmacological effects on the tissue heterogeneity and vulnerability (to wave breaks and re-entry) are quantified to show that drugs that increase the wavelength and stop re-entry (I_{K1} and I_{Kur} blockers) can also increase the heterogeneity (AP gradients of 26–27 ms) and the likelihood of wave breaks.

Conclusion Biophysical modelling reveals large conduction block areas near the PVs, which are due to discontinuous fibre arrangement enhanced by electrical heterogeneity. Vulnerability to re-entry in such areas can be modulated by pharmacological interventions.

Keywords Atrial arrhythmias • Pulmonary veins • Computational modelling • Re-entrant waves • Drug effects

Introduction

Atrial fibrillation (AF) self-perpetuates by multifactor electrical remodelling in the atria, which can explain the high prevalence and treatment-resistant nature of this commonest sustained arrhythmia. The myocardial sleeves of the pulmonary veins (PVs) extending into the left atrium (LA) have been recognized as the primary sources of high-frequency electrical activity during AF, and PV ablation is routinely used to terminate AF clinically.[1–3] However, mechanisms by which the PVs can sustain arrhythmogenic activity are unclear, and its clinical treatments have significant intrinsic limitations.[3]

Experimental[4,5] and computational[6,7] studies of the PV sleeves in animal models reveal substantial electrical heterogeneities and complex arrangements of myocardial fibres resulting in conduction discontinuities and unstable re-entrant waves. Similar activation patterns have been observed at the PV-LA junctions during catheter mapping in AF patients,[8,9] leading to suggestions that high-frequency activity in the PV can be sustained by re-entry.[2,3,8] Stable re-entrant

* Corresponding author. Tel: +44 20 7188 7188 (ext. 53217), fax: +44 20 718 85442, E-mail: oleg.aslanidi@kcl.ac.uk

What's new?

- Electrophysiologically and anatomically detailed 3D model of the pulmonary veins developed to study the effects of electrical tissue remodelling and anti-arrhythmic drugs;
- Electrical heterogeneity and conduction anisotropy of the pulmonary veins both contribute to the generation of pro-arrhythmogenic conduction blocks and wave breaks;
- Cell-to-cell coupling reduction decreases the conduction velocity and increases the likelihood of wave breaks, but the linked wavelength decrease is not sufficient for sustained re-entry;
- Ion channel remodelling (associated with atrial fibrillation) substantially decreases the action potential duration and wavelength, and therefore promotes the sustenance of re-entry;
- Potassium channel current blockers can terminate re-entry by increasing the action potential duration and wavelength, but promote wave breaks by increasing electrical heterogeneity;
- Amiodarone can both terminate re-entry and reduce the likelihood of wave breaks by substantially decreasing tissue heterogeneity and vulnerability to conduction block.

patterns have recently been simulated using computational models of the human atria:[10] the study has demonstrated effects of electrical remodelling on AF self-perpetuation by re-entry, but did not consider anisotropy of the PVs.

Multiple experimental studies have shown that AF-induced electrical remodelling is characterized by decreases in atrial action potential duration (APD),[9–11] which are associated with underlying changes to the expression of several membrane ion channels reported both in dog[11,12] and human.[13–15] At the tissue level, remodelling has also been linked with down-regulation and heterogeneous expression of connexin proteins that form intercellular gap junctions (responsible for the AP conduction), as well as the presence of severe fibrosis and fibre disorganization.[16–18] The latter factors may contribute to decreases in the AP conduction velocity (CV)[19] and increases in conduction anisotropy[4] during AF.

A lack of mechanistic understanding of factors underlying AF onset and evolution may explain relatively low success rates in its clinical treatment, with ~30–50% recurrence even after expensive ablation and cardioversion procedures.[20,21] Available anti-arrhythmic drug therapies for AF also have moderate effectiveness and risk of life-threatening proarrhythmic complications.[22] Knowledge of the underlying mechanisms may assist in tailoring the drug therapies to the evolving AF dynamics, and hence in increasing the efficacy and safety of pharmacological treatments for various AF cases. Biophysically detailed models can help to dissect such electro-pharmacological mechanisms.[23–25]

In this study, we apply a detailed electrically heterogeneous and anisotropic model of the canine PV region[6] to (i) incorporate effects on ion channel and gap junction remodelling seen in chronic AF in dog;[11,12,19] (ii) investigate the evolution of arrhythmic re-entrant substrate for AF due to such effects, and (iii) dissect potential pharmacological interventions that can terminate the re-entrant activity.

Methods

Single cell models

The Ramirez–Nattel–Courtemanche[26] model is used to simulate the ion channel currents contributing to the AP of a single canine atrial myocyte. This model is modified to incorporate detailed the current density data specific to the canine LA and PV cells (*Figure 1* and Table 1), as in a previous study.[27] The resultant AP in the PV cell has a shorter APD and more positive resting potential than the LA cell (*Figure 1B*). Atrial fibrillation-induced electrical remodelling is also incorporated into the model based on experimental ion channel current measurements from dog[12] (Table 1). This involves a reduction of the conductance of the L-type calcium channel current, I_{CaL}, by 50%, a reduction of the conductance of the transient outward potassium channel current, I_{to}, of 55% and an increase in the conductance of the voltage-dependant potassium channel current, I_{K1}, of 100%. Such modifications are consistent with those observed in human, wherein there are more available data.[10,14,15] A previous study has demonstrated the important role that remodelling of the ultra-rapid potassium channel current, I_{Kur}, may play in the behaviour of AF in electrophysiologically heterogeneous human atrial tissue.[10] Because I_{Kur} is atrial-specific, it may be particularly relevant to drug studies where it can be targeted without any adverse effects on the ventricles. Therefore remodelling of this ion channel is also included in the canine cell models. Due to a lack of available canine data regarding remodelling of this current, a 50% reduction of I_{Kur} (Table 1) is incorporated, which is consistent with data from human.[28,29] Ion channel remodelling shortens the APD of both cell models (Table 1) and reduces the LA-PV heterogeneity.

Three-dimensional tissue model

To simulate electrical activity in the PV at the tissue scale, a previously developed three-dimensional (3D) anatomical model of the canine PVs and inter-pulmonary region of the posterior LA[6] is used (*Figure 1A*). This model includes fine details of the fibre micro-architecture in this region, attained from high-resolution micro-CT images (*Figure 1C* and *D*). Details of the reconstruction have been described previously.[6,30] Importantly for this study, abrupt changes in the fibre arrangements are observed at junctions of the PVs and LA, such as the ostium of the left superior pulmonary vein (LSPV) (*Figure 1D*). Similar abrupt changes have been observed in experimental electro-anatomical studies.[4,31]

Action potential conduction is simulated by solving the mono-domain equation[32] on a 3D tissue geometry grid, as described previously.[6,33] Conduction anisotropy, defined as the ratio between diffusion coefficients (characterizing electrotonic cell-to-cell coupling) in the longitudinal and transverse fibre directions, is 16 : 1 in the PVs and 10 : 1 in the LA. These correspond to experimentally validated CV values in the PV and LA tissue regions.[6] Cell-to-cell coupling reduction is introduced by decreasing the diffusion coefficients by 50%. This corresponds to the abbreviation in AP conduction velocities associated with AF, experimentally observed to be around 10–40% in various stages of remodelling.[17,18] In the 3D model, this resulted in decreases of the maximum longitudinal CV from 1.25 to 0.75 m/s and the minimum transverse CV from 0.31 to 0.21 m/s. Note that atrial tissue remodelling can be underlain by multiple pathophysiological factors, such as down-regulation and heterogeneous expression of gap junction proteins, atrial dilatation, and fibrosis. However, establishing links with the specific factors was beyond the scope of this study.

Vulnerability to re-entry

Vulnerability to the initiation and sustenance of re-entrant waves underlying AF is analysed by measuring the time vulnerability windows to

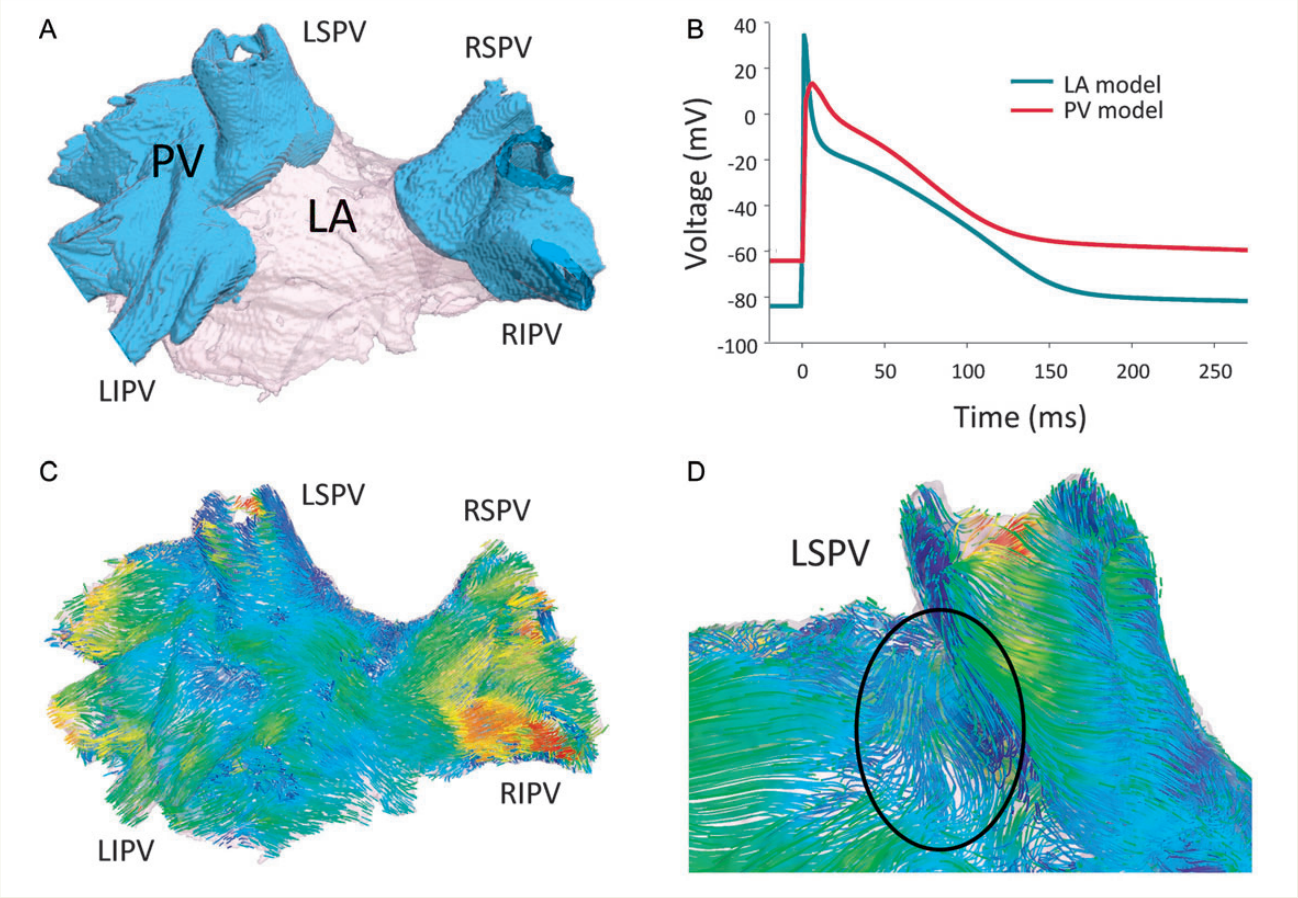

Figure 1 Model of the canine PV region. (*A*) Three-dimensional segmented geometry, the PV and LA regions are indicated by different colours and labelled. (*B*) Segmentation-specific APs in the LA and PV regions. (*C*) Fibre orientation in the PV region, atrial fibres are tracked and coloured according to the main local fibre orientation component along the anterior-posterior direction.[6] (*D*) Fibre discontinuities near the LSPV ostium. PV, pulmonary veins, LSPV, left superior pulmonary vein; LIPV, left inferior pulmonary vein; RSPV, right superior pulmonary vein; RIPV, right inferior pulmonary vein.

Table 1 Electrical heterogeneity and remodelling in the PV-LA region[a]

	$I_{Ca,L}$ (pA/pF)	I_{K1} (pA/pF)	I_{to} (pA/pF)	I_{Ks} (pA/pF)	I_{Kur} (pA/pF)	APD (ms)
LA control	8.0 (8.5)	5.0 (5.8)	9.0 (8.4)	5.0 (5.3)	10.0	185 (195)
PV control	6.0 (5.9)	3.5 (3.6)	4.5 (5.6)	9.0 (9.8)	10.0	173 (175)
LA remodelled	4.0 (3.4)	10.0 (9.3)	4.0 (3.6)	5.0 (5.0)	5.0	112 (125)
PV remodelled	3.0 (2.6)	7.0 (6.1)	2.0 (2.8)	9.0 (9.8)	5.0	107 (130)

[a]Ion channel current densities and APDs for the PV and LA cell models under control and full remodelling conditions. Simulated values are in good agreement with the respective experimental values[12] shown in brackets. Note that the current density of I_{Kur} (step current) in control is the same as in the original paper by Ramirez *et al.*[26] The current density of I_{Kur} in remodelling conditions is halved as seen in human atrial cells.[10]

conduction block leading to (i) at least a single wave break (VW_{CB}) and (ii) re-entry sustained over several rotations (VW_R). An S1-S2 pacing protocol is applied to a site combining substantial electrical heterogeneity (such as the LA-PV junction seen in *Figure 1A*) and structural anisotropy (such as the LSPV region indicated in *Figure 1D*), as has been suggested in previous studies in canine,[6] human[10,33] and rabbit.[34] Three S1 stimuli are applied at a cycle length of 280 ms, followed by a short-coupled S2 stimulus. The range of S2 stimuli coupling intervals for which an AP can propagate in one region (such as the PVs) but is blocked in the other (LA) is considered as the VW_{CB}. Within this window, the range of S2 stimuli coupling intervals for which this conduction block develops into sustained re-entry (lasting more than 4 s[10]) is considered the VW_R.

Vulnerability windows are assessed in multiple conditions to dissect the relative roles of ion channel remodelling, reduced cell-to-cell coupling, electrical heterogeneity and structural anisotropy in the development of re-entry. The following conditions are considered: control, full

Table 2 Drug effects on the APD of the PV and LA cell models in the ion channel remodelling case[a]

	Control	Remodelling	Remodelling + I_{K1} blocker	Remodelling + I_{Kur} blocker	Remodelling + amiodarone
LA APD (ms)	185	112	189	138	92
PV APD (ms)	173	107	163	111	89
ΔAPD (ms)	12	5	26	27	3

[a]Drug effect on the electrical heterogeneity between the PV and LA cells is also quantified as ΔAPD.

electrical remodelling (ion channel remodelling and cell-to-cell coupling reduction), ion channel remodelling only, cell-to-cell coupling reduction only, full remodelling without heterogeneity and full remodelling without anisotropy. Heterogeneity is removed by considering all 3D tissue geometry points as PV cells. As a result, differences in both the APD and resting potential between the LA and PV tissue (*Figure 1B*) are eliminated. Anisotropy is removed by setting the anisotropy ratio to 1 : 1 and adjusting the diffusion coefficient such that the overall activation time is comparable to control.[6]

Pharmacological effects

Models also incorporate the effects of pharmacological ion channel blockers, to study their potential effectiveness in the prevention and termination of re-entry. Up-regulation of I_{K1} associated with AF-induced remodelling has been shown to be a primary factor in the APD abbreviation.[35] Hence, this current provides a natural target for reversing the effects of AF-induced electrical remodelling. Due to the atrial-specific nature of I_{Kur}, this channel also presents an attractive target for a potential treatment of AF. Along with I_{K1} and I_{Kur} blockade, we also investigate effects of amiodarone, an exemplary multi-channel blocker that has proved effective in the treatment of AF.[36] Effects of I_{K1} and I_{Kur} blockers are simulated by reducing their conductances by 50% each. Effects of amiodarone are simulated by reducing the conductance of I_{CaL} and I_{Ks} by 40 and 50%, respectively.[37,38] Drug effects on the APD and its heterogeneity between the PV and LA cells are summarized in Table 2.

To study the relative effectiveness of various pharmacological agents on the prevention of re-entry in different AF cases, we quantify their effects on the VW_{CB} and VW_R in two conditions: (i) full remodelling and (ii) cell-to-cell coupling reduction only. In these two cases, the pharmacological effects are introduced from the beginning of the respective simulations. To study the effectiveness of various pharmacological agents in the termination of re-entry, their effects are introduced in a separate set of simulations after 4 s of sustained re-entrant activity.

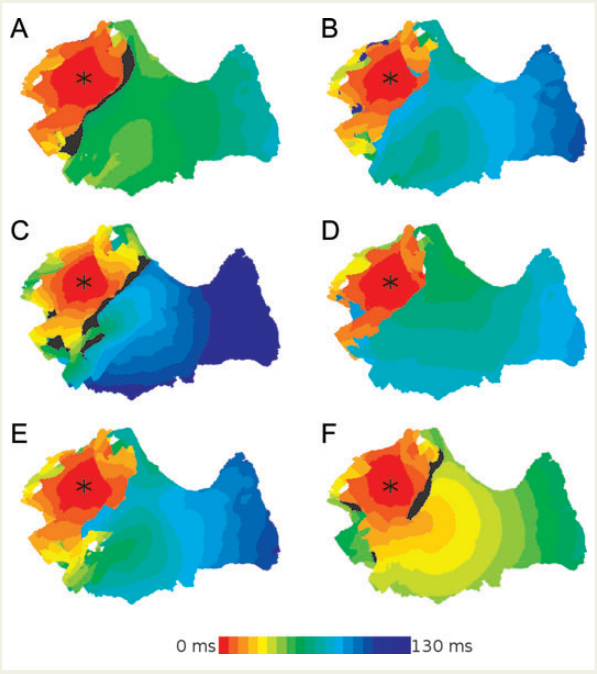

Figure 2 Generation of conduction blocks in the PV region. Simulated activation patterns following the LSPV pacing are shown for different conditions. (*A*) Control, (*B*) full remodelling, (*C*) cell-to-cell coupling reduction only, (*D*) ion channel remodelling only, (*E*) full remodelling without heterogeneity, (*F*) full remodelling without anisotropy. All activation times are measured from the time of the applied S2 stimulus. Regions coloured in black indicate areas in which excitation failed to propagate. The asterisk indicates the location of the applied stimuli.

Results

Generation of wave breaks and re-entry

Pacing in the anisotropic and heterogeneous site near the LSPV resulted in various patterns of wave propagation through the PV region (*Figure 2*). These simulations show that all factors considered (ion channel remodelling, cell-to-cell coupling reduction, heterogeneity, anisotropy) are important in the initiation and sustenance of re-entry. Each of these factors alone can result in conduction block and wave breaks, although activation patterns (*Figure 2*) and VW_{CB} (Table 3) are quantitatively different. However, only the combination of these factors can result in sustained re-entry (Table 3). In such a combination, electrical heterogeneity and anisotropy promote a relatively large VW_{CB}, ion channel remodelling results in a decreased effective refractory period (ERP, linked to the APD), and coupling reduction results in a decreased CV. The short wavelength (WL = ERP × CV) promotes the development of sustained re-entry from the initial conduction block and wave breaks.

In control (*Figure 2A*), conduction block of a wave spreading from the LSPV towards the LA occurs within a large VW_{CB} (18 ms, Table 3). However, the relatively fast CV and long wavelength (0.78 m/s and 171 mm, respectively) prevent the wave breaks from re-entering the LSPV region and generating a complete re-entrant circuit. With full remodelling (*Figure 2B*), the same pacing protocol can generate sustained re-entry. The combination of remodelled electrical heterogeneity (5 ms, Table 2) and anisotropy results in a

Table 3 Vulnerability of the PV tissue to re-entry initiation (VW_{CB}) and sustenance (VW_R)[a]

	VW_{CB} (ms)	VW_R (ms)	WL (mm)
Control (no remodelling)	221–239	–	171
Cell-to-cell coupling reduction only	215–243	–	102
Ion channel remodelling only	105–115	–	81
Full remodelling (ion channel + coupling)	103–115	107–109	49
Full remodelling, isotropic tissue	103–110	–	49
Full remodelling, homogeneous tissue	103–111	103	49
Full remodelling + I_{Kur} blocker	111–128	–	53
Full remodelling + I_{K1} blocker	145–167	–	68
Full remodelling + amiodarone	97–101	–	46
Cell-to-cell coupling reduction + I_{Kur} blocker	222–246	–	105
Cell-to-cell coupling reduction + I_{K1} blocker	335–368	–	159
Cell-to-cell coupling reduction + amiodarone	167–183	–	79

[a]The vulnerability windows are quantified under various conditions and under effects of various pharmacological agents. The wavelength is measured as WL = ERP × CV, where ERP corresponds to the lower bound of the VW_{CB}.

substantial VW_{CB} (7 ms, Table 3), whereas the decreased velocity and wavelength (0.47 m/s and 49 mm, respectively) allow for the wave breaks to complete and sustain a re-entrant circuit. The mechanisms of transition from the initial conduction block to sustained re-entry (through specific re-entrant conduction pathways) are discussed in the next section.

With cell-to-cell coupling reduction only, re-entry cannot be initiated (*Figure 2C*). The CV is clearly reduced compared to control (see in *Figures 2A* and *C*), but the wavelength is not further reduced due to he absence of ion channel remodelling (Table 3). Therefore, the PVs do not fully recover at the time the wave returns to the region of initial conduction block, and re-entry fails. With ion channel remodelling only (*Figure 2D*), sustained re-entry cannot be initiated. The short APD (Table 2)—and hence, decreased ERP and wavelength (Table 3)—allows for a single re-entrant circuit to be completed, but the relatively fast CV due to the intact cell-to-cell coupling means the wavelength is still too long to permit sustained re-entry. Hence, quick self termination of the re-entrant circuit occurs. Note that VW_{CB} is much wider in the cell-to-cell coupling reduction case compared to ion channel remodelling (Table 3), and hence the reduced coupling is more favourable for the generation of wave breaks (*Figure 2C*). However, ion channel remodelling is more favourable for re-entry (*Figure 2B* and *D*). Each component of full electrical remodelling provides more substrate for re-entry than control.

Both electrical heterogeneity and anisotropy contribute to the generation of conduction block and the propagation pattern promoting sustained re-entry (*Figure 2E* and *F*). Thus, the largest VW_{CB} and VW_R are observed in the full remodelling condition in the presence of both anisotropy and heterogeneity: if either heterogeneity or anisotropy is removed, VW_{CB} is decreased and VW_R largely disappears (Table 3). If heterogeneity is removed, the abrupt fibre angle change observed at the junction of the PVs and LA by the LSPV (*Figure 1D*) is sufficient to result in a conduction block in this region (*Figure 2E*). Within a very small window (<1 ms, Table 3) this conduction block can develop into sustained re-entry. When anisotropy is removed, sustained re-entry cannot be initiated (*Figure 2F*). Note that VW_{CB} is very similar in the anisotropic and homogeneous cases (Table 3). Therefore, both the fibre arrangement and electrical heterogeneity may play an equally important role in the development of wave breaks.

Transition from wave breaks to re-entry

Transition from wave breaks (arising from a conduction block near the PVs) to stable, sustained re-entry is illustrated in *Figure 3*. Primarily, an S2 stimulus applied near the LSPV results in the AP propagating within the PVs, but blocked from entering the LA (*Figure 3Ai*). As described in the previous section, the conduction block occurs at the LSPV site that combines large electrical heterogeneity and anisotropy. The wave propagates around the block line to the superior part of the LSPV and the inferior part of the LIPV (*Figure 3Ai*). These directions are largely determined by the fibre orientation patterns seen in *Figure 1C* and *D*. The AP propagates along fibre bundles wrapped around the LSPV and LIPV, eventually entering into the LA from the posterior and inferior directions (*Figure 3Aii*). The time needed for the waves to propagate around the PVs is sufficient for the LA tissue to recover, hence allowing the waves to propagate into this region (*Figure 3Aiii*). The wave then propagates back towards the site of initial conduction block, where it re-enters the PVs and travels towards the initiation site (*Figure 3Aiii* and *iv*). Afterwards, the same re-entrant pattern is repeated, with the waves following the same conduction pathways around the LSPV and LIPV (*Figure 3B*). This transitional re-entrant pattern is observed within the first second of simulation (*Figure 3Ci*). However, after several seconds only a single dominant re-entrant wave is sustained around the LIPV (*Figure 3Cii*), whereas the second wave is suppressed.

Anti- and pro-arrhythmic drug effects

Application of each ion channel blocker had a significant effect on the wave behaviour. Sustained re-entry initiated in the full remodelling condition (*Figure 3*) was terminated by the application of I_{K1} (but not I_{Kur}) channel blocker or amiodarone after 4 s of simulating the

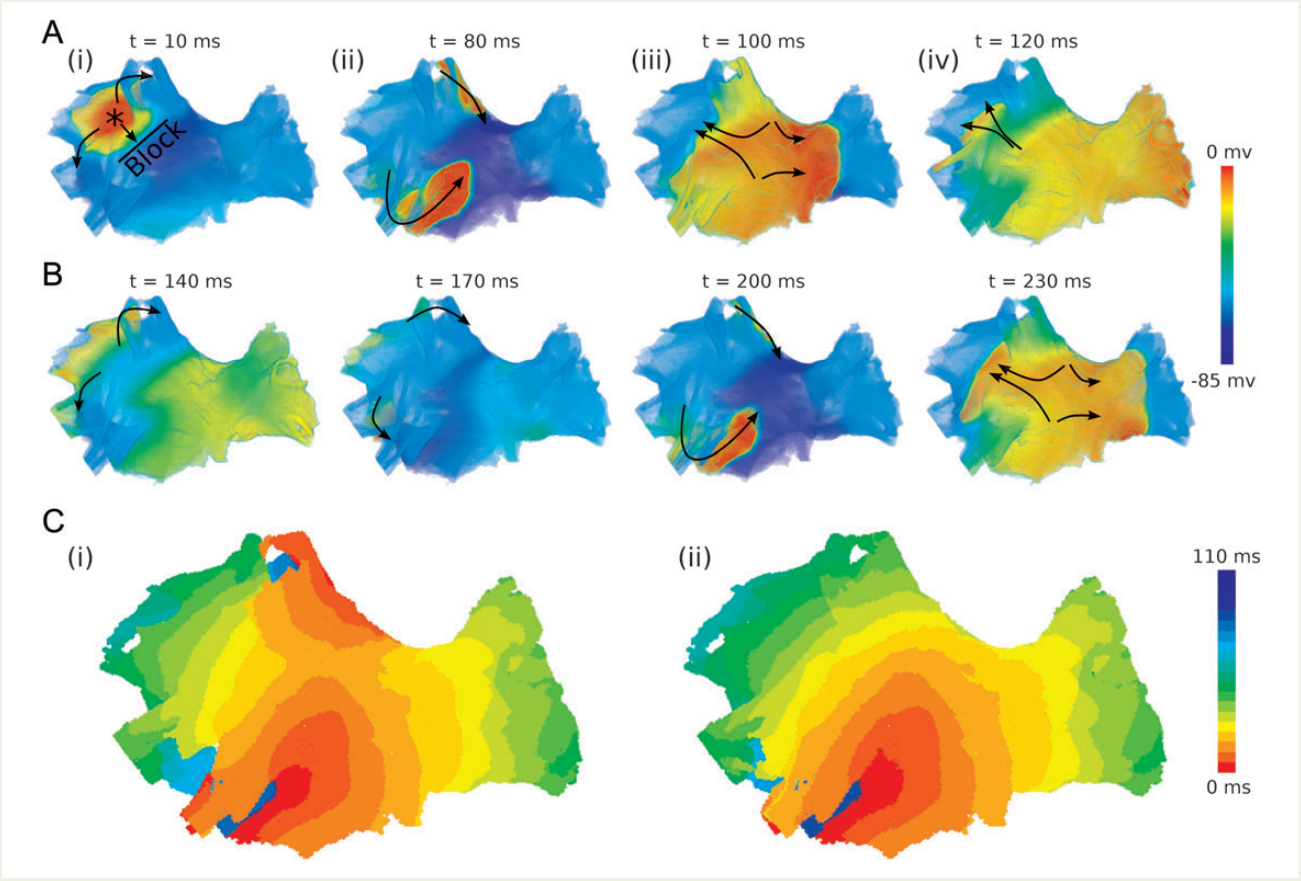

Figure 3 Generation of sustained re-entry in the PV region. Snapshots of re-entrant waves and the resultant activation patterns are shown. (*A*) and (*B*) Initiation and sustenance of re-entry. Timings indicated are following the S2 stimulus. Arrows indicate direction of wavefront propagation. (*C*) Activation patterns during the transient (i) and sustained (ii) rotations of a stable re-entrant wave.

stable re-entrant rotation. Sustained re-entry could not be generated in the full remodelling condition with the application of either I_{Kur} or I_{K1} channel blockers or amiodarone (Table 3) at the start of 5 s simulations.

However, effects of the pharmacological agents on the generation of wave breaks were different. Blocking either I_{Kur} or I_{K1} increased the wavelength, but also increased the extent of the VW_{CB} (Table 3). Thus, blocking I_{Kur} and I_{K1} increased the VW_{CB} from 12 to 17 and 22 ms, respectively. Therefore, both these channel blockers displayed anti-arrhythmogenic effects through increasing the wavelength and decreasing the likelihood of sustained re-entry, but pro-arrhythmogenic effects through increasing the electrical heterogeneity (Table 2) and likelihood of conduction blocks and wave breaks (Table 3). Note that conduction block lines and multiple wavelets have been linked primarily with chronic AF.[39,40]

Amiodarone was the only drug considered without apparent pro-arrhythmogenic effects. Apart from preventing the generation and sustenance of re-entry (see above), it also substantially decreased the VW_{CB} from 12 to 4 ms (Table 3), therefore decreasing the likelihood of wave break generation. This is consistent with the clinically observed superiority of amiodarone over other drugs used for AF treatment.[15,24,36] The underlying electrophysiological mechanism can be based on the reduction of APD differences between the PV and LA cells by amiodarone (Table 2). As shown above, such electrical heterogeneity is important in the generation of both wave breaks (Table 3) and re-entry (*Figure 2E*).

Note that the same drugs can result in different wave behaviours in different AF cases—thus, drug effects in the cell-to-cell coupling reduction only case result in very different ERPs and VWs (Table 3).

Discussion

Simulations of a biophysically detailed 3D model of the canine PV region show that a combination of factors is needed to generate re-entrant waves: (i) electrical heterogeneity and conduction anisotropy can lead to pro-arrhythmogenic conduction block lines and wave breaks; (ii) cell-to-cell coupling reduction decreases the CV and increases the likelihood of such wave breaks, but does not provide a substrate for sustained re-entry; (iii) ion channel remodelling decreases the ERP and promotes the sustenance of re-entry; (iv) I_{Kur} blockers can prevent the generation of transient re-entry, but cannot prevent the generation of wave breaks or terminate sustained re-entry; (v) I_{K1} blockers can effectively eliminate re-entrant substrate by substantially increasing the ERP, but also increase the likelihood of pro-arrhythmogenic wave breaks by increasing the electrical heterogeneity; and (vi) amiodarone can both eliminate re-entrant activity and decrease the likelihood of wave breaks.

These results are in agreement with previous experimental and computational studies. Blockers of repolarising K^+ channel currents are known to reduce effectively the re-entrant substrate size by increasing the APD and wavelength.[24] However, currently available anti-arrhythmic drugs are only moderately effective in preventing or terminating AF, and may also exert adverse effects.[15] Our study may explain such adverse effects by the increases of the VW_{CB} and the likelihood of wave breaks in response to blocking I_{K1} and I_{Kur}. Such wave breaks (rather than re-entry) have been linked with chronic AF.[39,40] This may explain experimental data showing that the inhibition of I_{Kur} can actually promote the induction of AF.[41] Our simulation results may also provide mechanistic insights into the clinically observed superiority of amiodarone over other drugs used for AF treatment,[15,24,36] as amiodarone uniquely reduces the likelihood of both re-entry and wave breaks (Table 3).

Results in this study are consistent with those of a previous computational study in humans.[10] In both studies, ion channel remodelling decreased but did not eliminate regional heterogeneity. The presence of electrical heterogeneity (Table 2) combined with the short wavelengths (Table 3) associated with both ion channel remodelling (decreased ERP) and cell-to-cell coupling reduction (decreased CV) promoted the development of stable high-frequency re-entrant circuits in both studies. Another previous study allowed for the first detailed investigation of the role of fibre anisotropy in the development and behaviour of re-entrant circuits in the PVs.[6] This study built upon the previous results[6,10] by combining detailed electrical heterogeneity and anisotropy in the PV region[6] with electrical remodeling,[10] as well as the pharmacological effects.[37] The results obtained allow us to dissect factors responsible for various aspects of wave dynamics underlying AF.

Interestingly, our new results for the first time clearly demonstrate that abrupt changes in fibre angle alone can produce conduction blocks, wave breaks and sustained re-entry (Table 3). Moreover, conduction pathways determined by the fibres provide the substrate for sustaining re-entry (*Figure 3*). These results are also supported by test simulations where the LA (rather than the PV) was fast-paced under the full remodelling condition. As a result of such pacing, an area of conduction block was observed between the LA and PV regions—this area had approximately the same location as the conduction block area seen during the PV pacing under same conditions (*Figure 2*), indicating the role of local fibre orientation. The VW_{CB} due to the LA pacing (108–116 ms) was smaller than that due to the PV pacing (103–115 ms), as in the latter case the anisotropy effect was enhanced by the PV-to-LA conduction against the APD gradient. Thus, the likelihood of wave breaks was lower during the LA pacing than the PV pacing, and no re-entry was observed during the LA pacing. More detailed studies are warranted to identify the most likely areas of re-entry initiation and sustenance in the 3D atria.

Limitations

This study considered the PV region only, as AF is commonly associated with this region.[1–7] However, it is important to consider the behaviour of re-entry within the PVs in the context of the entire atria. This would enable investigation of the evolution of waves driven by the PVs at the organ scale, and would also provide a much larger substrate for wave propagation and re-entry. This may change the effectiveness of the drugs in terminating re-entry in the entire atria. For example, I_{K1} block was successful in terminating re-entry by increasing the wavelength. Within the small physical substrate of the PVs, the re-entrant wave did not have sufficient space to perpetuate, and hence self terminated. The effect on re-entry perpetuation may be different at the larger whole atria scale. A biophysically detailed model for the entire 3D canine atria is currently being developed.[42] Note also that the regional PV model enables more time efficient study of local tissue properties (such as VW_{CB}). Similar studies using the entire 3D atria models can be very expensive computationally.

It is also important to note a simple nature of the models of drug actions. This study did not consider drug binding kinetics or dose dependencies,[43] as well as potential adverse effects on the other parts on the heart.[22] Such details were not required to achieve the aims of this study. Our simulation results are in good agreement with cell-to-tissue level electro-pharmacological data,[24,36] and may provide useful insights into the effects of drugs on wave dynamics underlying AF. Moreover, cell-to-cell coupling reduction in this study was uniform, and the CV changes were not linked with AF-induced increases in conduction anisotropy and levels of fibrosis.[16–18] Careful consideration should also be given to multiple cell electrophysiology factors (such as relative contributions of the APD and resting potential to electrical heterogeneity), as well as differences between the single cell and intact tissue experimental data used in the models.[12,44,45] Quantifying all these factors and incorporating them into 3D models could provide a big challenge for both experimental and computational studies of the mechanisms of AF sustenance.

Conclusion

The complexity of mechanisms and large variability in pathophysiological factors underlying AF make it likely that distinctive and often several therapeutic options will be needed for individual AF cases. In this study, we have applied computational modelling for studying the evolution and pharmacological modulation of wave dynamics in the PV tissue under conditions of AF-induced remodelling. Simulation results demonstrated that ion channel remodelling and cell-to-cell coupling reduction both reduce the wavelength and promote the development of stable re-entrant circuits, while preserving the substantial electrical heterogeneity and anisotropy to create the asymmetries necessary for the initiation of wave breaks and re-entry. Elimination of individual factors (such as atrial heterogeneity, anisotropy, ion remodelling, cell-to-cell-coupling reduction) can lead to the termination of re-entry, but multiple wave breaks still persist. Pharmacological modulation of the electrical heterogeneity and vulnerability are also quantified to show that specific drugs that eliminate re-entry (an anti-arrhythmic effect) can at the same time increase the likelihood of wave breaks (a pro-arrhythmic effect). As 3D atrial models incorporate increasingly realistic anatomical and functional parameters linked to the development of AF, this should improve our understanding of electrophysiological mechanisms of complex wave behaviours underlying various AF cases, as well as their pharmacological prevention.

Acknowledgements

The authors acknowledge support from the National Institute for Health Research (NIHR) comprehensive Biomedical Research

Centre award to Guy's & St Thomas' NHS Foundation Trust in partnership with King's College London and King's College Hospital NHS Foundation Trust.

Conflict of interest: none declared.

Funding

This work was funded by a project grant (PG/10/69/28524) from the British Heart Foundation.

References

1. Haïssaguerre M, Jaïs P, Shah DC, Takahashi A, Hocini M, Quiniou G *et al.* Spontaneous initiation of atrial fibrillation by ectopic beats originating in the pulmonary veins. *N Engl J Med* 1998;**339**:659–66.
2. Nattel S, Shiroshita-Takeshita A, Brundel BJ, Rivard L. Mechanisms of atrial fibrillation: lessons from animal models. *Prog Cardiovasc Dis* 2005;**48**:9–28.
3. Calkins H, Kuck KH, Cappato R, Brugada J, Camm AJ, Chen S-A *et al.* 2012 HRS/EHRA/ECAS expert consensus statement on catheter and surgical ablation of atrial fibrillation: recommendations for patient selection, procedural techniques, patient management and follow-up, definitions, endpoints, and research trial design. *Europace* 2012;**14**:528–606.
4. Hocini M, Ho SY, Kawara T, Linnenbank AC, Potse M, Shah D *et al.* Electrical conduction in canine pulmonary veins: electrophysiological and anatomic correlation. *Circulation* 2002;**105**:2442–8.
5. Arora R, Verheule S, Scott L, Navarrete A, Katari V, Wilson E *et al.* Arrhythmogenic substrate of the pulmonary veins assessed by high-resolution optical mapping. *Circulation* 2003;**107**:1816–21.
6. Aslanidi OV, Colman MA, Varela M, Zhao J, Smaill BH, Hancox JC *et al.* Heterogeneous and anisotropic integrative model of pulmonary veins: computational study of arrhythmogenic substrate for atrial fibrillation. *Interface Focus* 2013;**3**:20120069.
7. Butters TD, Aslanidi OV, Zhao J, Smaill B, Zhang H. A novel computational sheep atria model for the study of atrial fibrillation. *Interface Focus* 2013;**3**:20120067.
8. Narayan SM, Krummen DE, Clopton P, Shivkumar K, Miller JM. Direct or coincidental elimination of stable rotors or focal sources may explain successful atrial fibrillation ablation: on-treatment analysis of the confirm (conventional ablation for AF with or without focal impulse and rotor modulation) trial. *J Am Coll Cardiol* 2013;**62**:138–47.
9. Kumagai K, Ogawa M, Noguchi H, Yasuda T, Nakashima H, Saku K. Electrophysiologic properties of pulmonary veins assessed using a multielectrode basket catheter. *J Am Coll Cardiol* 2004;**43**:2281–9.
10. Colman MA, Aslanidi OV, Kharche S, Boyett MR, Garratt CJ, Hancox JC *et al.* Pro-arrhythmogenic effects of atrial fibrillation induced electrical remodelling-insights from 3D virtual human atria. *J Physiol* 2013;**591**:4249–72.
11. Fareh S, Villemaire C, Nattel S. Importance of refractoriness heterogeneity in the enhanced vulnerability to atrial fibrillation induction caused by tachycardia-induced atrial electrical remodeling. *Circulation* 1998;**98**:2202–9.
12. Cha T-J, Ehrlich JR, Zhang L, Chartier D, Leung TK, Nattel S. Atrial tachycardia remodeling of pulmonary vein cardiomyocytes: comparison with left atrium and potential relation to arrhythmogenesis. *Circulation* 2005;**111**:728–35.
13. Van Wagoner DR, Nerbonne JM. Molecular basis of electrical remodeling in atrial fibrillation. *J Mol Cell Cardiol* 2000;**32**:1101–17.
14. Workman AJ, Kane KA, Rankin AC. The contribution of ionic currents to changes in refractoriness of human atrial myocytes associated with chronic atrial fibrillation. *Cardiovasc Res* 2001;**52**:226–35.
15. Dobrev D, Ravens U. Remodeling of cardiomyocyte ion channels in human atrial fibrillation. *Basic Res Cardiol* 2003;**98**:137–48.
16. Ausma J, Wijffels M, Thoné F, Wouters L, Allessie M, Borgers M. Structural changes of atrial myocardium due to sustained atrial fibrillation in the goat. *Circulation* 1997;**96**:3157–63.
17. Van der Velden HMW, Jongsma HJ. Cardiac gap junctions and connexins: their role in atrial fibrillation and potential as therapeutic targets. *Cardiovasc Res* 2002;**54**:270–9.
18. Severs NJ, Coppen SR, Dupont E, Yeh H-I, Ko Y-S, Matsushita T. Gap junction alterations in human cardiac disease. *Cardiovasc Res* 2004;**62**:368–77.
19. Gaspo R, Bosch RF, Talajic M, Nattel S. Functional mechanisms underlying tachycardia-induced sustained atrial fibrillation in a chronic dog model. *Circulation* 1997;**96**:4027–35.
20. Camm AJ, Kirchhof P, Lip GYH, Schotten U, Savelieva I, Ernst S *et al.* Guidelines for the management of atrial fibrillation: the task force for the management of atrial fibrillation of the European Society of Cardiology (ESC). *Europace* 2010;**12**:1360–420.
21. Weerasooriya R, Khairy P, Litalien J, Macle L, Hocini M, Sacher F *et al.* Catheter ablation for atrial fibrillation: are results maintained at 5 years of follow-up? *J Am Coll Cardiol* 2011;**57**:160–6.
22. Dobrev D, Nattel S. New antiarrhythmic drugs for treatment of atrial fibrillation. *Lancet* 2010;**375**:1212–23.
23. Noble D. Computational models of the heart and their use in assessing the actions of drugs. *J Pharmacol Sci* 2008;**107**:107–17.
24. Workman AJ, Smith GL, Rankin AC. Mechanisms of termination and prevention of atrial fibrillation by drug therapy. *Pharmacol Ther* 2011;**131**:221–41.
25. Zemzemi N, Bernabeu MO, Saiz J, Cooper J, Pathmanathan P, Mirams GR *et al.* Computational assessment of drug-induced effects on the electrocardiogram: from ion channel to body surface potentials. *Br J Pharmacol* 2013;**168**:718–33.
26. Ramirez RJ, Nattel S, Courtemanche M. Mathematical analysis of canine atrial action potentials: rate, regional factors, and electrical remodeling. *Am J Physiol Heart Circ Physiol* 2000;**279**:H1767–85.
27. Aslanidi OV, Butters TD, Ren CX, Ryecroft G, Zhang H. Electrophysiological models for the heterogeneous canine atria: computational platform for studying rapid atrial arrhythmias. *Conf Proc IEEE Eng Med Biol Soc* 2011;**2011**:1693–6.
28. Caballero R, de la Fuente MG, Gómez R, Barana A, Amorós I, Dolz-Gaitón P *et al.* In humans, chronic atrial fibrillation decreases the transient outward current and ultrarapid component of the delayed rectifier current differentially on each atria and increases the slow component of the delayed rectifier current in both. *J Am Coll Cardiol* 2010;**55**:2346–54.
29. Christ T, Boknik P, Wöhrl S, Wettwer E, Graf EM, Bosch RF *et al.* L-type Ca^{2+} current downregulation in chronic human atrial fibrillation is associated with increased activity of protein phosphatases. *Circulation* 2004;**110**:2651–7.
30. Aslanidi OV, Nikolaidou T, Zhao J, Smaill BH, Gilbert SH, Holden AV *et al.* Application of micro-computed tomography with iodine staining to cardiac imaging, segmentation, and computational model development. *IEEE Trans Med Imaging* 2013;**32**:8–17.
31. Ho SY, Cabrera JA, Sanchez-Quintana D. Left atrial anatomy revisited. *Circ Arrhythm Electrophysiol* 2012;**5**:220–8.
32. Clayton RH, Bernus O, Cherry EM, Dierckx H, Fenton FH, Mirabella L *et al.* Models of cardiac tissue electrophysiology: progress, challenges and open questions. *Prog Biophys Mol Biol* 2011;**104**:22–48.
33. Aslanidi OV, Colman MA, Stott J, Dobrzynski H, Boyett MR, Holden AV *et al.* 3D virtual human atria: a computational platform for studying clinical atrial fibrillation. *Prog Biophys Mol Biol* 2011;**107**:156–68.
34. Aslanidi OV, Boyett MR, Dobrzynski H, Li J, Zhang H. Mechanisms of transition from normal to reentrant electrical activity in a model of rabbit atrial tissue: interaction of tissue heterogeneity and anisotropy. *Biophys J* 2009;**96**:798–817.
35. Zhang H, Garratt CJ, Zhu J, Holden AV. Role of up-regulation of I_{K1} in action potential shortening associated with atrial fibrillation in humans. *Cardiovasc Res* 2005;**66**:493–502.
36. Shinagawa K, Shiroshita-Takeshita A, Schram G, Nattel S. Effects of antiarrhythmic drugs on fibrillation in the remodeled atrium insights into the mechanism of the superior efficacy of amiodarone. *Circulation* 2003;**107**:1440–6.
37. Benson AP, Aslanidi OV, Zhang H, Holden AV. The canine virtual ventricular wall: a platform for dissecting pharmacological effects on propagation and arrhythmogenesis. *Prog Biophys Mol Biol* 2008;**96**:187–208.
38. Holden AV, Aslanidi OV, Benson AP, Clayton RH, Halley G, Li P *et al.* The virtual ventricular wall: a tool for exploring cardiac propagation and arrhythmogenesis. *J Biol Phys* 2006;**32**:355–68.
39. Allessie MA, de Groot NMS, Houben RPM, Schotten U, Boersma E, Smeets JL *et al.* Electropathological substrate of long-standing persistent atrial fibrillation in patients with structural heart disease: longitudinal dissociation. *Circ Arrhythm Electrophysiol* 2010;**3**:606–15.
40. Verheule S, Tuyls E, van Hunnik A, Kuiper M, Schotten U, Allessie M. Fibrillatory conduction in the atrial free walls of goats in persistent and permanent atrial fibrillation. *Circ Arrhythm Electrophysiol* 2010;**3**:590–9.
41. Burashnikov A, Antzelevitch C. Can inhibition of IKur promote atrial fibrillation? *Heart Rhythm* 2008;**5**:1304–9.
42. Varela M, Zhao J, Aslanidi OV. Determination of atrial myofibre orientation using structure tensor analysis for biophysical modelling. *Lect Note Comput Sci* 2013;**7954**:425–32.
43. Davies MR, Mistry HB, Hussein L, Pollard CE, Valentin J-P, Swinton J *et al.* An *in silico* canine cardiac midmyocardial action potential duration model as a tool for early drug safety assessment. *Am J Physiol Heart Circ Physiol* 2012;**302**:H1466–80.
44. Miyauchi Y, Hayashi H, Miyauchi M, Okuyama Y, Mandel WJ, Chen PS *et al.* Heterogeneous pulmonary vein myocardial cell repolarization implications for reentry and triggered activity. *Heart Rhythm* 2005;**2**:1339–45.
45. Ehrlich JR, Cha TJ, Zhang L, Chartier D, Melnyk P, Hohnloser SH *et al.* Cellular electrophysiology of canine pulmonary vein cardiomyocytes: action potential and ionic current properties. *J Physiol* 2003;**551**:801–13.